JACS
JOURNAL OF THE AMERICAN CHEMICAL SOCIETY

Article

pubs.acs.org/JACS

Tight Binding of Carboxylate, Phosphonate, and Carbamate Anions to Stoichiometric CdSe Nanocrystals

Peter E. Chen, Nicholas C. Anderson, Zachariah M. Norman, and Jonathan S. Owen*

Department of Chemistry, Columbia University, 3000 Broadway, MC 3121, New York, New York 10027, United States

Supporting Information

ABSTRACT: To completely displace the carboxylate surface ligands from cadmium selenide nanocrystals, oleic acid impurities are first removed using dimethylcadmium or diethylzinc. In addition to metal carboxylate and methane coproducts, reactions with $CdMe_2$ produce surface bound methyl groups (δ = 0.4 ppm, 0.04−0.22 nm^{-2}) that photolytically dissociate to methyl radicals and *n*-doped nanocrystals. Without oleic acid impurities, cadmium carboxylate can be completely displaced from the surface using *n*-alkylamines (NH_2R', R′ = *n*-butyl, *n*-hexyl, *n*-octyl) (≤0.01 carboxylates nm^{-2}). Colloidal dispersions of amine bound nanocrystals (CdSe−NH_2R') are indefinitely stable at amine concentrations of 0.1 M or higher and slowly aggregate at lower concentrations. Dissociation and evaporation of the amine ligands in 4-ethylpyridine, tri-*n*-butylphosphine, or molten tri-*n*-octylphosphine oxide solution results in nanocrystal aggregation. CdSe−NH_2R' reacts with oleic acid, *n*-octadecylphosphonic acid, or carbon dioxide to form surface bound *n*-alkylammonium oleate, phosphonate, and carbamate ion pairs that bind with greater affinity than primary *n*-alkylamines. The results indicate that nanocrystal dispersions solely stabilized by neutral donor ligands are relatively unstable compared to those stabilized by adsorbed metal carboxylate or phosphonate complexes or by ion pairs. The challenge of differentiating between the neutral ligand bound form and adsorbed ion pairs is discussed.

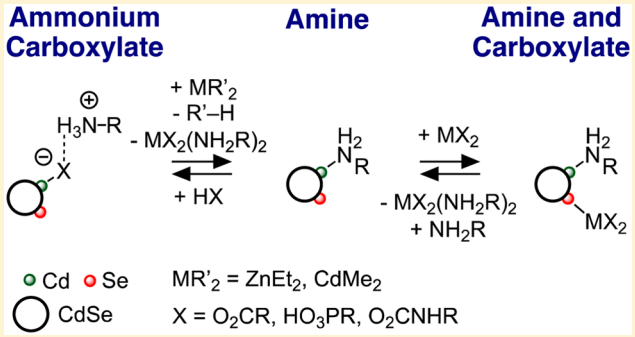

INTRODUCTION

Early strategies to exchange the ligands bound to cadmium selenide nanocrystals focused on neutral donors, such as tri-*n*-octylphosphine oxide (TOPO). However, more recent studies conclude that surface bound metal carboxylate and phosphonate complexes or adsorbed ion pairs are the more dominant ligand types (I, Scheme 1).[1,2] Exchanging these ligands has required reagents that cleave the metal carboxylate or metal phosphonate linkage, such as trialkyloxonium salts[3−6] or silyl and ammonium chalcogenides[7−9] and halides.[10−12] In most cases, these approaches produce electrostatically stabilized dispersions in polar solvents where a surface bound cation or anion balances charge with an outer sphere counterion (II, Scheme 1). The surface bound ions provide a valuable avenue to tailor nanocrystal properties; however, the counterions can lead to capacitive currents, low charge transport mobilities, and hysteretic transport properties.[8,13−15] Nonetheless, electrostatically stabilized nanocrystals have enabled rapid progress in the fabrication of nanocrystal photovoltaics and thin-film transistors with record-breaking performance in recent years.[16,17]

On the other hand, well-characterized nanocrystals solely stabilized by neutral ligands are rare. In many cases, samples that were thought to be stabilized by neutral donors, including TOPO[18] and primary *n*-alkylamines,[19,20] are actually stabilized by impurities such as phosphonate and phosphinate anions or *n*-alkylammonium-*N*-*n*-alkylcarbamate salts formed from primary amines and carbon dioxide (III, Scheme 1).[20]

In principle, a nanocrystal bound solely by labile neutral donors could be obtained by completely displacing adsorbed anions or surface bound metal complexes using Lewis bases.[21] However, previous attempts to do so using *n*-alkylamines,[22−24] phosphines,[22] and pyridine[25−29] consistently report partial ligand exchange with a small fraction (10−15%)[28,29] of the ligands proving difficult to remove. Recent work on the displacement of cadmium carboxylate ligands from zincblende cadmium selenide nanocrystals found that diamines and primary *n*-alkylamines are effective displacement reagents, removing as much as 90−95% of the ligand shell as measured in situ using ^{1}H nuclear magnetic resonance (NMR) spectroscopy. However, even following repeated cycles of displacement and purification under optimized conditions, 3−10% of the starting carboxylate ligands remain.[21]

Although the nature of the tightly bound fraction of carboxylate was unclear at the outset of our study, we reasoned that it might derive from an adsorbed ammonium carboxylate ion pair formed from an amine and a carboxylic acid (III, Scheme 1). Our hypothesis arose from a recent study of ligand cleavage using trimethylsilyl chloride, where protic impurities in

Received: December 23, 2016
Published: January 26, 2017

DOI: 10.1021/jacs.6b13234
J. Am. Chem. Soc. 2017, 139, 3227−3236

Scheme 1. Common Modes of Stabilizing a Colloidal Dispersion[a]

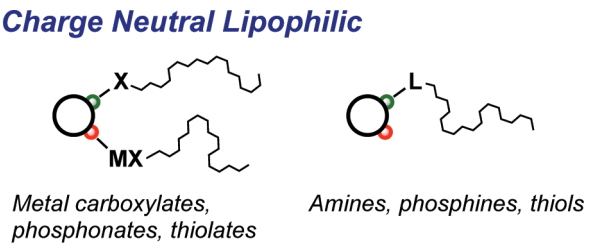

[a]Key: white, stoichiometric metal chalcogenide nanocrystal; red, surface selenium; green, surface cadmium.

the starting carboxylate terminated nanocrystals (CdSe–$Cd(O_2CR)_2$) led to the formation and adsorption of hydrochloride salts: tri-*n*-butylphosphonium chloride and *n*-butylammonium chloride.[10] These same protic impurities could also complicate the displacement of cadmium carboxylate. For example, addition of *n*-alkylamines to carboxylate terminated CdSe nanocrystals containing a carboxylic acid impurity (CdSe–$Cd(O_2CR)_2/HO_2CR$) could form *n*-alkylammonium and carboxylate ions that bind the nanocrystal (Scheme 2). If both ions remain inner sphere, it would be difficult to distinguish an adsorbed ammonium carboxylate ion pair from amine and cadmium carboxylate ligands.

In principle, the adsorption of ammonium carboxylate and ammonium phosphonate salts could explain reports of partial ligand exchange when amines are used as displacement reagents, provided that their affinity for the surface is strong. To test this hypothesis, we developed a method to scavenge

Scheme 2. Formation of Surface Bound Ammonium Carboxylate Ion Pairs[a]

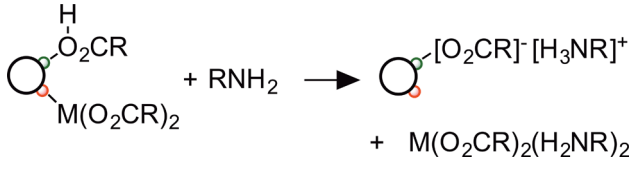

[a]Key: white, stoichiometric metal chalcogenide nanocrystal; red, surface selenium, green, surface cadmium.

carboxylic acids and other acidic impurities from CdSe–$Cd(O_2CR)_2/HO_2CR$ using dimethylcadmium ($CdMe_2$) or diethylzinc ($ZnEt_2$). With these nanocrystals, we investigated the subsequent displacement of their $Cd(O_2CR)_2$ surface ligands and successfully isolated nanocrystals bound solely by *n*-alkylamines (CdSe–NH_2R', R′ = *n*-butyl, *n*-hexyl, *n*-octyl). CdSe–NH_2R' is reactive toward ligand exchange as well as the formation of adsorbed carboxylate, phosphonate, and carbamate ion pairs upon reaction with carboxylic or phosphonic acid or carbon dioxide. Our studies show that neutral donor ligands provide relatively weak stabilization compared to adsorbed ion pairs or metal phosphonates or carboxylate complexes.

RESULTS AND DISCUSSION

Reaction of CdSe–$Cd(O_2CR)_2/HO_2CR$ with $CdMe_2$. Addition of $CdMe_2$ to CdSe–$Cd(O_2CR)_2/HO_2CR$ causes the immediate formation of methane (δ = 0.16 ppm) as observed in situ using ^{1}H NMR spectroscopy. After 24 h, unreacted $CdMe_2$ (bp = 105.5 °C) can be removed under vacuum leaving nanocrystals with surface bound methyl groups CdSe–$Cd(O_2CR)_2/CdMe_2$ that can be detected by a broad ^{1}H NMR resonance of low intensity in benzene-d_6 solution (δ = 0.4 ppm, 0.15 nm^{-2}, ~7 per nanocrystal, see below) (Figure 1). To the best of our knowledge, this is the first report of metal chalcogenide nanocrystals with metal–alkyl ligands.

Photolysis of CdSe–$Cd(O_2CR)_2/CdMe_2$ eliminates the broad ^{1}H NMR signal from surface bound methyl groups and produces CH_4 (δ = 0.2 ppm) in benzene-d_6 and a mixture of CH_4 and CH_3D in tetrahydrofuran-d_8 solution (Figures S1 and S2).[30] Photolysis also reduces the extinction of the lowest energy excitonic transitions in the UV–vis absorbance spectrum and quenches the photoluminescence (Figure 2).

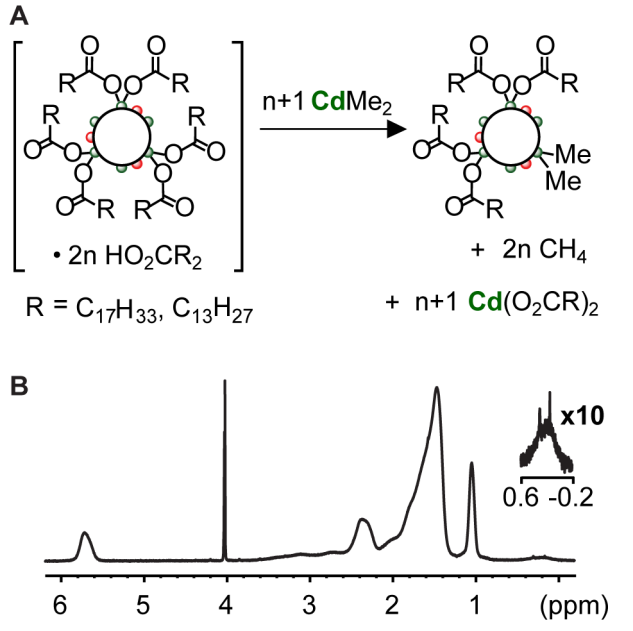

Figure 1. (A) Reaction of CdSe–$Cd(O_2CR)_2/HO_2CR$ with $CdMe_2$ methylates the nanocrystal surface. Key: white, stoichiometric metal chalcogenide nanocrystal; red, surface selenium; green, surface cadmium. (B) ^{1}H NMR spectrum of the product nanocrystals showing resonances from carboxylate ligands, a ferrocene internal standard (δ = 4 ppm), as a well as a broad signal from surface bound methyl groups (δ = 0.4 ppm).

DOI: 10.1021/jacs.6b13234
J. Am. Chem. Soc. 2017, 139, 3227–3236

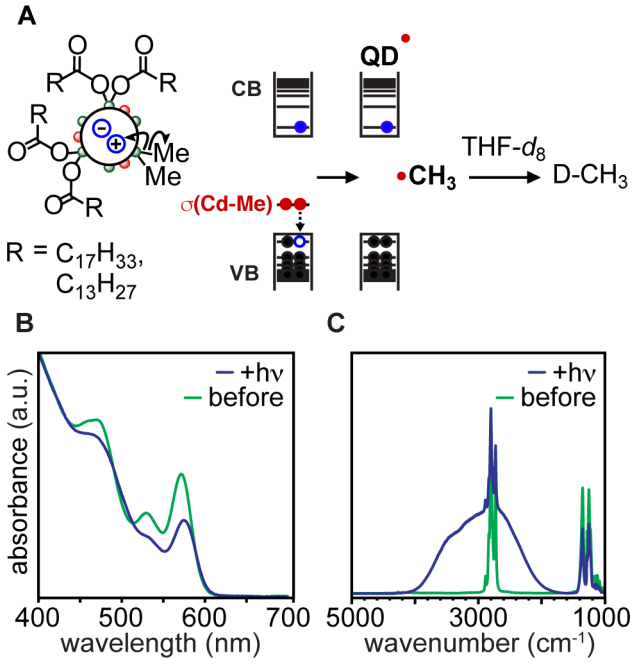

Figure 2. (A) Reaction scheme illustrating hole trapping at a Cd−Me bond and liberation of a methyl radical as well as an *n*-doped nanocrystal (QD•). Hydrogen atom abstraction from the solvent produces CH_3D. Key: white, stoichiometric metal chalcogenide nanocrystal; red, surface selenium; green, surface cadmium. (B) UV−vis absorption spectra illustrating the change in the excitonic features before (green) and after (blue) photolysis. (C) Infrared absorption spectra before (green) and after (blue) photolysis showing an intraband absorption feature that is coincident with (C−H) stretching bands.

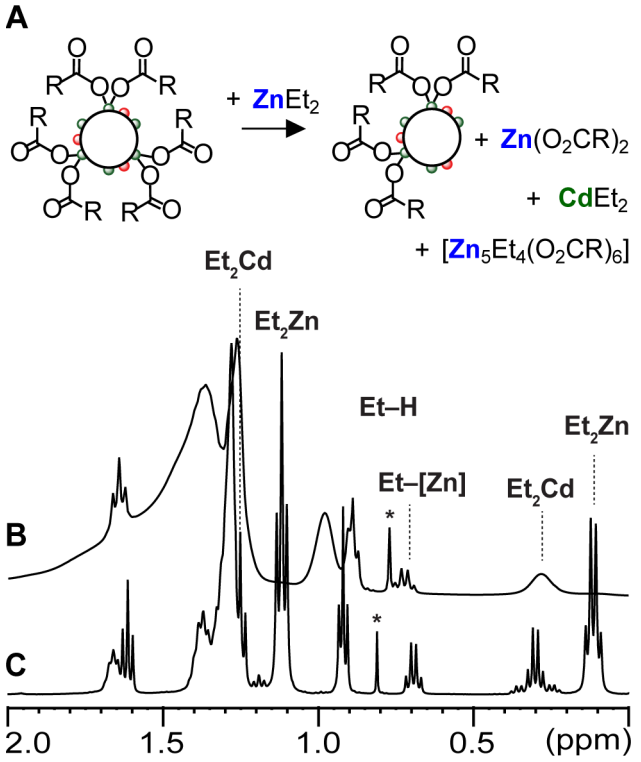

Figure 3. (A) Reaction of CdSe−Cd$(O_2CR)_2$/HO_2CR with $ZnEt_2$ leads to $CdEt_2$ and Zn$(O_2CR)_2$. Key: white, stoichiometric metal chalcogenide nanocrystal; red, surface selenium; green, surface cadmium. (B) ^{1}H NMR spectrum of reaction between CdSe−Cd$(O_2CR)_2$/HO_2CR and $ZnEt_2$. (*) is assigned to ethane. Unlabeled signals are from carboxyl chains bound to the nanocrystal or free in solution. (C) ^{1}H NMR spectrum of the reaction between Cd$(O_2CR)_2$ and $ZnEt_2$ in benzene-d_6. $^{111/113}$Cd satellites can be seen surrounding both signals from the methylene and the methyl groups of $CdEt_2$ (δ = 0.30 and 1.25 ppm).

At the same time, an intraband absorption feature appears in the infrared spectral range (ν = 2000−4000 cm^{-1}). Both are characteristic of a nanocrystal containing electrons in its conduction band.[31−34] Exposure of the sample to air or UV light (Figure S3) recovers the absorbance and photoluminescence properties of the starting CdSe−Cd$(O_2CR)_2$, presumably because dioxygen oxidizes the reduced nanocrystal. Related spectroscopic changes have been reported upon exposure of nanocrystals to triethyl borohydride, sodium biphenyl, and other reductants.[33,35,36] We conclude that the photoexcited nanocrystal oxidizes the surface bound methyl groups, eliminating methyl radicals that abstract a hydrogen or deuterium atom from the carboxylate ligands or the tetrahydrofuran-d_8 solvent.

Reaction of CdSe−Cd$(O_2CR)_2$/HO_2CR with $ZnEt_2$. Addition of $ZnEt_2$ to CdSe−Cd$(O_2CR)_2$/HO_2CR causes the immediate formation of ethane (δ = 0.8 ppm) and photochemical reduction of the nanocrystals (Figure S4). However, after removal of the volatiles, no NMR signals from surface bound ethyl groups could be observed. During the preparation of this manuscript, a related study also reported photochemical reduction of CdSe nanocrystals in the presence of $ZnEt_2$.[36]

Interestingly, addition of $ZnEt_2$ (2 equiv/carboxylate) to CdSe−Cd$(O_2CR)_2$/HO_2CR induces desorption of ∼50% of the carboxyl ligands and produces $CdEt_2$ (Figure 3). In addition, a new quartet is visible that is upfield of typical aliphatic resonances (δ = 0.7−0.9 ppm). We tentatively assign this resonance to the methylene fragment of a pentanuclear zinc cluster, $Zn_5Et_4(O_2CR)_6$, on the basis of its chemical shift, the lack of Cd satellites, and an analogous structurally characterized cluster ($Zn_5Et_4(OAc)_6$) that forms upon conproportionation of zinc acetate and $ZnEt_2$.[37] An independent study of the reaction between $ZnEt_2$ and cadmium oleate also produces $CdEt_2$, which matches the chemical shift and J_{Cd-H} couplings reported earlier (δ = 1.25 ppm, $^3J_{Cd-H}$ = 30 Hz, δ = 0.3 ppm, $^2J_{Cd-H}$ = 50 Hz).[38,39] After removal of the volatiles under vacuum and precipitation of the nanocrystals from toluene, zinc and oleate ligands can be recovered from the supernatant as verified using Fourier transform infrared (FT-IR), ^{1}H NMR, and energy dispersive X-ray spectroscopies (Figure S5). These observations indicate that $ZnEt_2$ and Cd$(O_2CR)_2$ undergo metathesis to $CdEt_2$, Zn$(O_2CR)_2$, and $Zn_5Et_4(O_2CR)_6$. We conclude that conversion of $ZnEt_2$ to Zn$(O_2CR)_2$ causes desorption of the carboxylate ligands, presumably because Zn$(O_2CR)_2$ and $Zn_5Et_4(O_2CR)_6$ have a weaker affinity for the cadmium selenide surface than does Cd$(O_2CR)_2$. The decreased carboxylate coverage helps explain the observed reduction in the PLQY from 10% to 2%.[21] A lower binding affinity of $CdEt_2$ compared to $CdMe_2$ might explain the lack of ^{1}H NMR signals from bound ethyl groups.

The rapid formation of ethane and methane upon addition of $ZnEt_2$ or $CdMe_2$ to CdSe−Cd$(O_2CR)_2$/HO_2CR supports the presence of an impurity sufficiently acidic to rapidly protonolyze the Zn−Et or Cd−Me bond. Integrating the ^{1}H NMR signals from the ethane and methane byproducts indicates the acidic impurity makes up 10 mol % of the ligand

DOI: 10.1021/jacs.6b13234
J. Am. Chem. Soc. 2017, 139, 3227−3236

shell. This quantity is consistent with our previous study of ligand exchange using trimethylsilyl chloride. We hypothesize that the oleic acid present in the ligand shell is the source of these acidic hydrogens (the presence of water was ruled out in our previous study by the lack of a bis-trimethylsilylether coproduct);[10] however, another protic impurity produced by the synthesis could also be involved.

Isolation of Stoichiometric Amine Bound Nanocrystals, CdSe–NH_2R'. Prior attempts to completely displace $Cd(O_2CR)_2$ from CdSe–$Cd(O_2CR)_2$/HO_2CR only partially eliminated the carboxylate ligands (to 0.3 nm^{-2}), results that were confirmed in this study using ^1H NMR spectroscopy as well as FT-IR spectroscopy to monitor a sharp ν(C–H) mode at 3005 cm^{-1} characteristic of the oleyl alkenyl group (Figure S6).[21,40] However, if acidic hydrogens are first removed using $ZnEt_2$ or $CdMe_2$, the carboxylate ligands can be completely displaced from the surface and amine bound nanocrystals isolated (oleate coverages $\leq$ 0.01 nm^{-2}) (Figure 4, S7).[41] Thus, the formation of tightly bound *n*-octylammonium oleate, can explain the difficulty of removing the final 0.3 nm^{-2} carboxylates from CdSe–$Cd(O_2CR)_2$/HO_2CR.

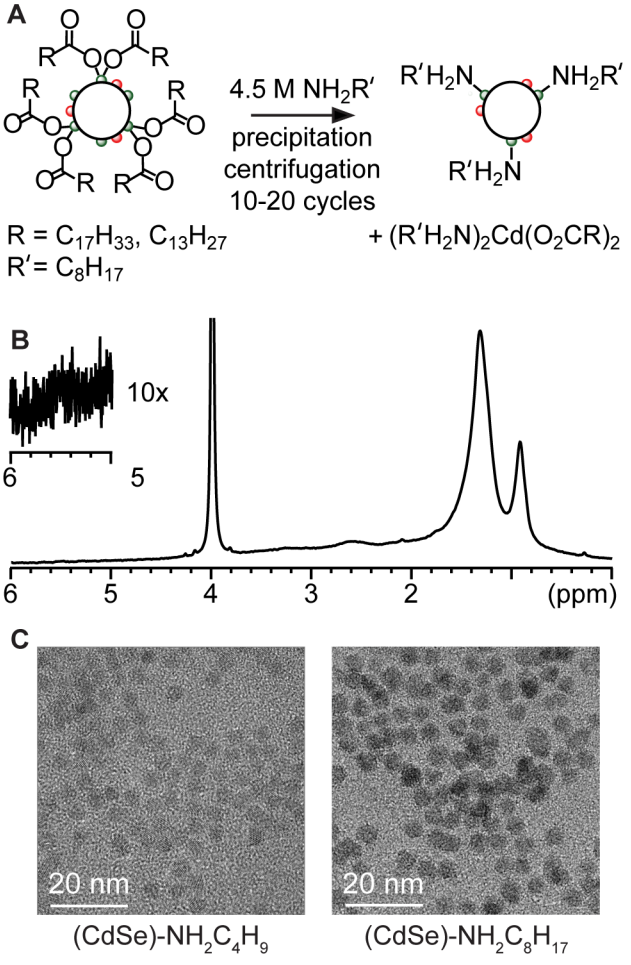

Figure 4. (A) Synthesis of CdSe–NH_2R' by displacement of $Cd(O_2CR)_2$ with primary amines. Key: white, stoichiometric metal chalcogenide nanocrystal; red, surface selenium; green, surface cadmium. (B) ^1H NMR spectrum of CdSe–NH_2R' in benzene-d_6. The inset shows the lack of an alkenyl resonance from oleate ligands. The signal at δ = 4 ppm is from ferrocene, which is used as an internal standard. (C) TEM images of CdSe–NH_2R' (R′ = *n*-butyl, *n*-octyl).

Interestingly, ^1H NMR spectra of CdSe–$Cd(O_2CR)_2$ dissolved in *n*-octylamine (4.5 M) and toluene-d_8 show that as much as 90% of the oleate ligands are freely tumbling in the amine solution (Figure S9a).[42] However, nanocrystals precipitated from this mixture retain roughly 50% of their original carboxylate coverage, and repeated precipitation of the nanocrystals from 4.5 M *n*-alkylamine solutions was required to completely separate *n*-butylamine and *n*-octylamine bound nanocrystals (CdSe–NH_2R', R = C_4H_9, C_8H_{17}) from cadmium carboxylate coproducts (see the Supporting Information). Attempts to improve the efficiency of the precipitation process by varying the amine structure, solvent mixture, reaction time, and concentration proved largely unsuccessful and will be described in detail elsewhere (Figure S9).

The amine ligands bound to CdSe–NH_2R' are labile at room temperature but effectively stabilize a colloidal dispersion that remains stable indefinitely provided that the amine concentration remains near 0.1 M or higher.[43] Although the kinetics of aggregation depend on a number of factors including nanocrystal concentration, solvent, and particle size, at amine concentrations lower than 0.1 M the nanocrystals begin to precipitate. Depending on the degree of aggregation, these precipitates can be partially redispersed upon stirring in *n*-alkylamine solution at 60 °C.

Transmission electron microscope (TEM) images of CdSe–NH_2R' (R′ = *n*-butyl, *n*-hexyl, *n*-octyl) prepared from 0.1 M amine solution show disordered aggregates regardless of the conditions used for the grid preparation or the amine chain length (Figure S10). However, UV–vis absorption and dynamic light scattering (DLS) measurements on nanocrystal dispersions are consistent with unaggregated nanocrystals (Figures S11 and S12). Moreover, when CdSe–NH_2R' is converted to CdSe–$Cd(O_2CR)_2$ by readsorption of $Cd(O_2CR)_2$, monolayers of well separated nanocrystals are visible using TEM (Figure S13). We conclude that CdSe–NH_2R' is unstable to aggregation, particularly when the sample is dried on a TEM grid.

Given the propensity of CdSe–NH_2R' to aggregate, we sought to test the stability of nanocrystal dispersions solely stabilized by other canonical Lewis basic surfactants, including 4-ethylpyridine, tri-*n*-butylphosphine (Bu_3P), and TOPO. CdSe–NH_2R' (where R′ = *n*-butyl) was added to Bu_3P or 4-ethylpyridine at room temperature or to molten TOPO at 50 °C, and stirred under dynamic vacuum to remove the *n*-butylamine ligands. In all cases, insoluble nanocrystal aggregates were obtained. While the aggregation kinetics depend on a number of factors including the nanocrystal concentration, solvent, and particle size, neither 4-ethylpyridine, Bu_3P, nor TOPO ligands stabilize a nanocrystal dispersion under neat conditions (>3 M). These results are surprising and suggest a clear difference between the nanocrystals prepared in this study and previous TOPO, Bu_3P, and pyridine stabilized dispersions (see below). One such difference is the use of zincblende nanocrystals in this study, while canonical CdSe nanocrystals typically have a wurtzite structure. In addition, previous reports of nanocrystal dispersions thought to be stabilized by TOPO, Bu_3P, and amines may also benefit from residual adsorbed metal surfactant complexes or carboxylate, phosphonate, or carbamate ion pairs.

Binding of Ammonium Oleate, Phosphonate, and Carbamate Ion Pairs. To further explore the binding of ammonium carboxylate to the nanocrystals, oleic acid (1 equiv/amine) was added to CdSe–NH_2R' (R = *n*-octyl, Scheme 3)

DOI: 10.1021/jacs.6b13234
J. Am. Chem. Soc. 2017, 139, 3227–3236

Scheme 3. Addition of Acidic Molecules to CdSe−NH_2R' Leads to Acid Dissociation and the Adsorption of an Ion Pair[a]

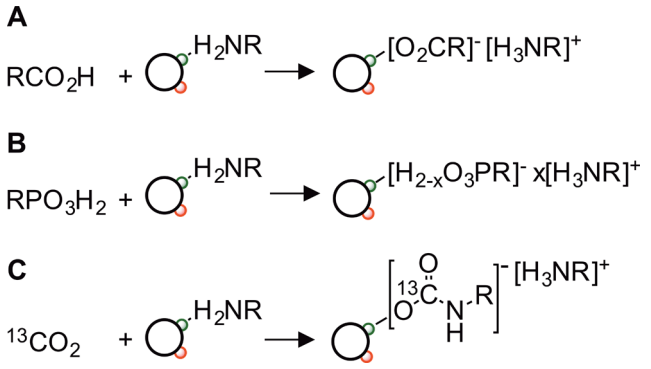

[a]Key: white, stoichiometric metal chalcogenide nanocrystal; red, surface selenium; green, surface cadmium.

and the product analyzed by ^{1}H NMR and FT-IR spectroscopies where signals characteristic of surface bound amine, ammonium, and oleate chains are visible (CdSe−NH_2R'/$[O_2CR]^-[H_3NR']^+$). Repeated precipitation from toluene only partially eliminates the broad ^{1}H NMR signals from bound carboxyl chains (to 0.59 nm^{-2}). In addition, a broad resonance centered at 7.5 ppm can be observed in the ^{1}H NMR spectrum (Figure S14), which is in the range previously reported for the $[H_3N-]^+$ fragment of *n*-alkylammonium species in the presence of metal oxide nanocrystals.[44]

FT-IR spectra of CdSe−NH_2R' show two distinct bands: (1) ν(C−H) = 2700−3000 cm^{-1} from alkyl chains and (2) a strong band for the coordinated amine (ν(N−H) = 3000−3400 cm^{-1}) that is absent in the spectrum of the pure amine ligand. Purified samples of CdSe−NH_2R'/$[O_2CR]^-[H_3NR']^+$ showed small differences in the region known to support ammonium stretching vibrations (ν(N−H) = 2700−3100 cm^{-1}), which overlaps with the ν(C−H).[45] However, the broad ν(N−H) band from the $[H_3N-]^+$ fragment is more clearly visible upon subtraction of a spectrum of CdSe−NH_2R' (Figure 5A,B). In addition, carboxylate stretching bands are visible ($\nu(CO_2)$) = 1408, 1564 cm^{-1}) that are distinct from oleic acid ($\nu(CO_2H)$) = 1710 cm^{-1}),[46] or a mixture of oleic acid and CdSe−$Cd(O_2CR)_2$ (ν = 1435, 1536, 1749 cm^{-1}) or the bending modes of CdSe−NH_2R' (ν = 1417, 1558 cm^{-1}). The retention of broad ^{1}H NMR signals and FT−IR bands from *n*-alkylammonium and oleate ligands following precipitation supports the formation and tight binding of ammonium oleate to the nanocrystal surface, despite the relatively high concentration of primary amines which might be expected to displace the carboxylate ligands.

In nonpolar solution, *n*-octylamine is not sufficiently basic to fully deprotonate a carboxylic acid as can be demonstrated using FT-IR spectroscopy (Figure S15).[47] Moreover, the low concentration of ammonium carboxylate ion pairs that do form are tightly associated via a hydrogen bond that is distinct from solvent separated ions in the FT-IR spectrum.[48] However, when oleic acid is added to CdSe−$NH_2C_8H_{17}$, the carboxylate and ammonium ions give unique signatures that support their binding to the surface as *n*-octylammonium oleate (0.59 nm^{-2}, Figure 5A). Similar adsorption of *n*-alkylammonium carboxylate ion pairs was observed in a study of hafnium oxide and cesium lead bromide nanocrystals;[2,44,49] however, the formation of ion pairs was not reported in a recent study of amine bound $CuInS_2$ nanocrystals.[50] Presumably, binding of the oleate anion to the Lewis acidic cadmium selenide, hafnium oxide, or cesium lead bromide surface stabilizes its negative charge, facilitating the proton transfer. Additionally, higher dielectric screening at the cadmium selenide surface might also play a role.[51,52]

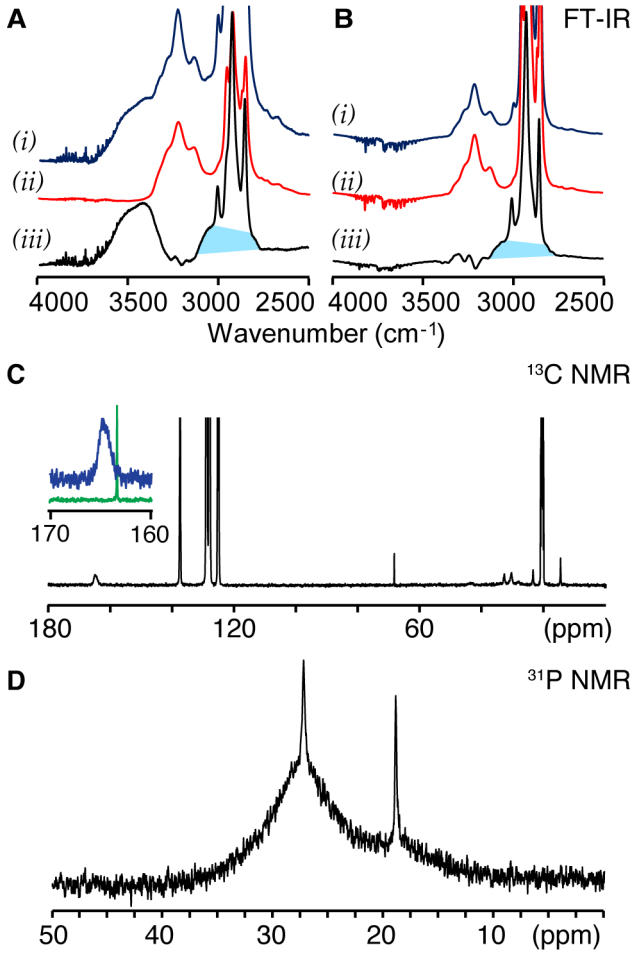

Figure 5. (A) FT-IR spectrum of (i) CdSe−NH_2R'/$[O_2CR]^-[H_3NR']^+$ (R = oleyl, R′ = *n*-octyl) prepared from oleic acid that had not been dried. A prominent water stretching band is visible (ν(O−H)) = 3300−3700 cm^{-1}), (ii) CdSe−NH_2R' (R′ = *n*-octyl), and (iii) their difference spectrum. $[H_3N]^+$ (ν(N−H)) highlighted in light blue. (B) FT-IR spectrum of (i) CdSe−NH_2R'/$[O_2CR]^-[H_3NR']^+$ (R = oleyl, R′ = *n*-octyl) prepared from anhydrous oleic acid, (ii) CdSe−NH_2R' (R′ = *n*-octyl), and (iii) their difference spectrum. $[H_3N]^+$ (ν(N−H)) highlighted in light blue. The spectra were normalized to amine ν(N−H) stretching band at 3200 cm^{-1} prior to subtraction. Spectra in (A) and spectra in (B) were obtained from samples with the same nanocrystal concentration. (C) ^{13}C NMR spectrum of reaction between CdSe−NH_2R' (R′ = *n*-octyl) and $^{13}CO_2$ ([*n*-octylamine] = 0.04 M, toluene-d_8). The inset shows the region from δ = 160−170 ppm where a broad resonance centered at 165 ppm corresponding to the carbamate carbon (blue) is visible and the same regions of a spectrum of *n*-octylammonium *N*-*n*-octylcarbamate in the absence of nanocrystals (green). (D) ^{31}P NMR spectrum of CdSe−NH_2R' (R′ = *n*-octyl). ([*n*-octylamine] = 0.021 M) and *n*-octadecylphosphonic acid 1 equiv./NH_2R'. Sharp and broad signals are assigned to free and bound *n*-octadecylphosphonate anions, respectively.

In order to test the generality of the ion pair formation and coordination, we added *n*-octadecylphosphonic acid to CdSe−NH_2R'. Two broad ^{31}P NMR resonances are observed that we

DOI: 10.1021/jacs.6b13234
J. Am. Chem. Soc. 2017, 139, 3227−3236

assign to surface bound monohydrogen *n*-octadecylphosphonate (δ = 27.2 ppm) and *n*-octadecylphosphonate (δ = 18.8 ppm) (Scheme 3 and Figure 5). *n*-Alkylphosphonic acids are sufficiently acidic to protonate *n*-alkylamines in the absence of nanocrystals, which we verified by an independent titration experiment (Figure S16).[53] Although a minor sharp signal overlays the broad resonances, we conclude the majority of the phosphonate anions bind the nanocrystal even in 0.02 M amine solution. This relatively strong binding helps explain the difficulty of displacing native phosphonic acid ligands from nanocrystals using amine donors.[54−56]

Carbon dioxide also reacts with CdSe−NH_2R', in this case leading to nanocrystals with amine and *n*-octylammonium-*N*-*n*-octylcarbamate ligands (CdSe−H_2NR'/[O_2C−$NHR']^-[H_3NR']^+$) (Scheme 3 and Figure 5). Liquid primary amines are known to dissolve significant quantities of carbon dioxide if stored under ambient conditions, leading to *n*-alkylammonium and *N*-*n*-alkylcarbamate ions that can dictate the outcome of nanocrystal syntheses that use amine surfactants.[19] Upon adding labeled carbon dioxide-^{13}C to a solution of CdSe−NH_2R', a broad ^{13}C NMR signal from the carbonyl carbon of a surface bound carbamate anion appears (δ = 165 ppm, $\Delta\delta$ = 1.95 ppm, 975 Hz). The FT-IR spectrum of CdSe−H_2NR'/[O_2C−$NHR']^-[H_3NR']^+$ also shows signals from *n*-octylammonium and *N*-*n*-octylcarbamate ions including three bands (ν = 3028, 3064, and 3087 cm^{-1}) that appear in an authentic sample of *n*-octylammonium *N*-*n*-octylcarbamate (Figure S17).[57−59]

Integration of the ^{13}C NMR signal (acquired using an inverse gated decoupling scheme) and comparing it to a natural abundance ferrocene standard shows that ∼0.1 carbamates nm^{-2} remain bound to the nanocrystal following one round of precipitation using methyl acetate. This coverage remains unchanged following three cycles of precipitation from concentrated *n*-octylamine solution (4.5 M). CdSe−NH_2R' or other nanocrystals stabilized by amine surfactants must, therefore, be stored free from air to avoid reaction with atmospheric carbon dioxide and contamination of the ligand shell.

The retention of surface bound *n*-alkylammonium oleate, carbamate, and phosphonate ion pairs following precipitation from amine solution signals their high affinity for the nanocrystal surface. Even in 4.5 M *n*-alkylamine solution, surface bound *n*-alkylammonium oleate is visible in the ^1H NMR spectrum. Moreover, their coverage only drops from 0.59 to 0.16 nm^{-2} following three cycles of precipitation from 4.5 M *n*-octylamine solution. These observations support an affinity that is much higher than primary *n*-alkylamines, a feature that may stem from their ability to chelate the surface.[60]

In the case of zincblende CdSe, the binding of the carboxylate is strongest on the [100] facets, which supports a multidentate bridging coordination mode involving adjacent cadmium centers.[61,62] The competitive binding of amines to these same sites is perhaps less favorable because the amine ligands are unlikely to bridge adjacent cadmium centers. Given that the density of atoms on this facet (5.9 nm^{-2}) is higher than the aerial packing density of crystalline *n*-alkane chains (4.9 nm^{-2}), complete coverage of this facet with one amine per cadmium atom will passivate only one of two dangling bonds at each cadmium center. On the other hand, each carboxylate ligand can passivate two to three binding sites per aliphatic chain, provided it binds in a η^2- or η^3-bridging bidentate mode (Scheme 4). Because of their chelating ability, we expect that

Scheme 4. Proposed Binding Modes of Carboxylate and Amine Ligands on [100] Facet of Zincblende Cadmium Chalcogenide Surface

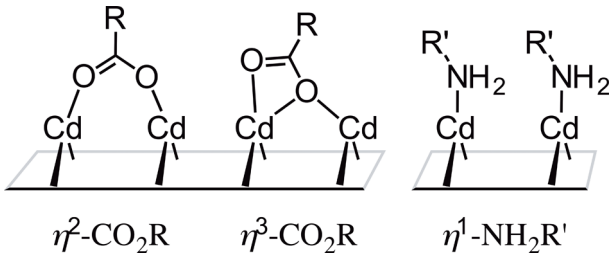

carboxylate, carbonate, and phosphonate ligands will have a greater affinity for the [100] facet than will primary *n*-alkylamines. This difference helps explain the persistent binding of these ligands in concentrated amine solution and points to a difference between zincblende and wurtzite structures, which lack a polar facet with analogous atomic structure.

Adsorption of Oleic Acid and Oleic Acid-d_1 to CdSe−Cd$(O_2CR)_2$. Our conclusion that *n*-alkylamines cause the formation of ammonium carboxylate ligands strongly suggests that oleic acid binds CdSe−Cd$(O_2CR)_2$ through several rounds of purification by precipitation from toluene with methyl acetate, a process that removes excess cadmium carboxylate. To confirm this finding, we added a large excess of oleic acid (400 equiv/nanocrystal) to a sample of CdSe−Cd$(O_2CR)_2$ that had first been reacted with $ZnEt_2$ and treated with TMEDA to reduce its oleate coverage (to 0.59 nm^{-2}) and the product characterized with ^1H NMR spectroscopy (see the Experimental Section). Five cycles of precipitation, centrifugation, and redissolution leave 1.14 oleate ligands nm^{-2}, or twice the initial coverage, which have a line width and diffusion constant that is consistent with bound ligands (Figures S21 and S22). Thus, ∼50% of the carboxyl ligands in this sample are oleic acid ligands and ∼50% derive from cadmium oleate.

The FT-IR spectrum of this independently prepared CdSe−Cd$(O_2CR)_2$/HO_2CR is indistinguishable from the starting CdSe−Cd$(O_2CR)_2$ with no carboxylic acid band (ν(C═O) = 1710 cm^{-1}) (Figure S23) and no signals from selenol (ν(Se−H) ∼ 2300 cm^{-1})[63] or hydroxyl (ν(O−H) ∼ 3000−4000 cm^{-1}) groups. A ^1H NMR signal from the acidic hydrogen could not be identified. Adsorption of oleic acid-d_1 (O−D) does not produce distinct FT-IR signals associated with the deuterium label nor a visible ^2H NMR signal. However, addition of $ZnEt_2$ to the labeled nanocrystals CdSe−Cd$(O_2CR)_2$/DO_2CR results in the formation of CH_2D−CH_3 (Figure S24). While the site of protonation is uncertain, it is clear that added oleic acid binds the nanocrystal and is not easily separated by precipitation.

Perspective. Among the modes of stabilizing a colloidal dispersion described in Scheme 1, the electric double layer formed by adsorbed ion pairs is perhaps most common. Sorption of ions on metal oxide surfaces in particular has been a subject of interest for decades.[64−66] Colloidal dispersions of organic micelles and polymer beads in aqueous media share a similar motif.[67] Likewise, recent examples of metal chalcogenide, metal oxide, metal, and metal halide nanocrystals have been synthesized with chalcogenide, thiocyanate, halide, citrate, or other polyanionic surface ligands that balance their charge with an outer sphere counterion and dissolve in polar media.[49,68−71] In the present case, however, we document examples where the counter cations are organic and the

DOI: 10.1021/jacs.6b13234
J. Am. Chem. Soc. 2017, 139, 3227−3236

nanocrystals remain soluble in nonpolar media such as toluene because of tight ion pairing with the surface bound anions. This mode of stabilization is well documented in the literature on metal nanocrystals where surfactants such as hexadecyltrimethylammonium bromide (CTAB) can stabilize dispersions of metal nanocrystals in toluene.[72] Our experiments show that carboxylate, phosphonate, and carbamate ions bind the nanocrystal tightly and are challenging to unambiguously distinguish from metal oleate and/or amine ligands. Moreover, the ease of forming these impurities from atmospheric carbon dioxide or acidic impurities in CdSe−$Cd(O_2CR)_2$/HO_2CR or so called TOPO capped nanocrystals suggests these adsorbed ions play a significant role in the chemistry of nanocrystals thought to be bound solely by amine ligands.

Many have proposed that pyridine and *n*-alkylamines, TOPO, and Bu_3P stabilize a colloidal dispersion of metal chalcogenide nanocrystals, yet the presence of undetected anions, such as octylphosphonate[18] and *n*-alkylcarbamate anions,[19,20] complicate these claims. While the poor stability of pyridine capped cadmium selenide is well documented,[24,73] other studies report stable dispersions of these nanocrystals in chloroform or pyridine solution.[24,74] In light of the incomplete displacement of native ligands using pyridine,[28,29] we speculate that the presence of adsorbed anions and pyridinium counter cations may have provided the stability in those cases. By comparison, the CdSe−NH_2R' isolated in this study is free from acidic impurities and adsorbed anions and aggregates in neat 4-ethylpyridine, TOPO, or Bu_3P.

Several observations made here indicate that *n*-alkylamine ligands also provide relatively weak stabilization: (1) the tendency of CdSe−NH_2R' to aggregate at low amine concentrations, (2) the well known lability of amine ligands on the ^{1}H NMR time scale (∼ms),[75] and (3) the complete desorption of amines from nanocrystal thin films.[76] We also conclude that ammonium carboxylate, phosphonate, or carbamate ion pairs bind the nanocrystals strongly and at low coverage more strongly than *n*-alkylamines, perhaps because of their ability to chelate the [100] surface. This may explain the difficulty of displacing the last few carboxylate or phosphonate ligands using amines and pyridine. Given the challenge of spectroscopically differentiating between an ammonium carboxylate ion pair and separate amine and carboxylate ligands, these findings suggest that surface bound ion pairs formed from amines are likely more pervasive than realized. More broadly, the formation of an adsorbed ion pair by deprotonation of an adventitious acid or displacement of a cationic metal complex provides a reasonable alternative to the simpler dative ligand−surface interaction. Such models are likely to be important for bulky N-heterocyclic carbenes[77−79] or multidentate ligands such as brush polymers with amine or imidazole terminated side chains[80] or polyvinylpyrrolidinone (PVP) where steric properties may prevent high density surface ligation.[81−83] Distinguishing between these modes of stabilization is essential to controlling ligand exchange reactivity by design.

CONCLUSION

The deprotonation of acidic molecules such as carboxylic acids, phosphonic acids, and carbamic acids is facilitated by the Lewis acidic surface of CdSe nanocrystals. The surface tightly binds the resultant carboxylate, phosphonate, and carbamate anions and prevents the complete displacement of the native ligands with primary amines. To address this limitation, we used $ZnEt_2$ and $CdMe_2$ to scavenge acidic hydrogens prior to displacing the surface metal oleate complexes. This strategy provides CdSe nanocrystals without anionic impurities, but the nanocrystals proved relatively unstable to aggregation unless the amine concentration was maintained near 0.1 M or higher. The stability worsens following exchange of the primary amine ligands for commonly used ligands such as 4-ethylpyridine, TOPO, or Bu_3P. These experiments show the somewhat surprising result that canonical neutral donor ligands do not effectively support stable colloidal dispersions. Moreover, it suggests that the stability of nanocrystals reported to be bound solely by neutral donor ligands, and amine ligands in particular, may benefit from the presence of acidic impurities that lead to adsorbed ion pairs.

EXPERIMENTAL SECTION

General Methods. Cadmium nitrate tetraaquo (99%), sodium hydroxide, myristic acid (99%), selenium dioxide (99.8%), anhydrous oleic acid (99%), 1-tetradecanol (95%), tri-*n*-butylphosphine (99%), methanol (99.8%), $^{13}CO_2$ (99% atom enriched, 1L lecture bottle), deuterium chloride (35 wt % in D_2O), and 1-octadecene (90%) were purchased from Sigma-Aldrich and used without further purification. Ferrocene (98%) was purchased from Sigma-Aldrich and purified by sublimation before use. Tri-*n*-octylphosphine oxide (99%) was purchased from Sigma-Aldrich and recrystallized from acetonitrile before use. Benzene-d_6 (99.6%), toluene-d_8 (99.5%), tetrahydrofuran-d_8 (99.5%), anhydrous acetonitrile (99.5%), anhydrous tetrachloroethylene (99%), and anhydrous methyl acetate (99.5%) were purchased from Sigma-Aldrich, shaken with activated alumina, filtered, and stored over 4 Å molecular sieves in an inert atmosphere glovebox at least 24 h prior to use. Pentane, tetrahydrofuran, and toluene were dried over alumina columns, shaken with activated alumina, filtered, and stored over 4 Å molecular sieves in an inert atmosphere glovebox at least 24 h prior to use. Dimethylcadmium and diethylzinc were purchased from Strem and vacuum distilled prior to use. *CAUTION: Me_2Cd is extremely toxic and because of its volatility and air sensitivity should only be handled by a highly trained and skilled researcher.* *N,N,N′,N′*-Tetramethylethylenediamine (TMEDA, 99.5%), 1,2-diaminocyclohexane (mixture of *cis* and *trans* isomers), *n*-octylamine (99%), *n*-hexylamine, and *n*-butylamine were purchased from Sigma-Aldrich and dried over CaH_2, distilled, and stored in a nitrogen glovebox. *n*-Octadecylphosphonic acid was synthesized as described previously.[84,85] Cadmium myristate and cadmium oleate were synthesized from $Cd(NO_3)_2{\cdot}4H_2O$ and the corresponding carboxylic acid on a 25 mmol scale following a modified procedure reported previously.[86]

All manipulations were performed under air-free conditions unless otherwise indicated using standard Schlenk techniques or within a nitrogen atmosphere glovebox. NMR spectra were recorded on Bruker Avance III 500 MHz instruments. ^{1}H NMR spectra were acquired with sufficient relaxation delay to allow complete relaxation between pulses (30 s). ^{13}C NMR spectra were collected using an inverse gated decoupling pulse program. ^{31}P NMR spectra were recorded with 2 s delays between pulses. DOSY measurements were performed using a double-stimulated echo sequence. The gradient strength was varied linearly from 2% to 95% of the probe's maximum value. The diffusion parameters consisting of the pulse length (δ/2) and delay (Δ) were chosen to ensure that >90% of the signal decayed at the highest magnetic field gradient. UV−vis data were obtained using a PerkinElmer Lambda 950 spectrophotometer equipped with deuterium and tungsten halogen lamps. Photoluminescence spectra and quantum yields were measured using a FluoroMax-4 equipped with an Integrating Sphere from Horiba Scientific according to a previous report.[21] FT-IR spectra were obtained using either a sodium chloride or lithium fluoride liquid cell in tetrachloroethylene with a Thermo Scientific Nicolet 6700 spectrometer equipped with a liquid N_2 cooled MCT-A detector.

Synthesis of CdSe−$Cd(O_2CR)_2$/HO_2CR. CdSe nanocrystals were synthesized using a previously reported procedure.[10,86] Purified

DOI: 10.1021/jacs.6b13234
J. Am. Chem. Soc. 2017, 139, 3227−3236

nanocrystals without ^{1}H NMR signals from free oleyl chains were used to make stock solutions in benzene-d_6 ([^-O_2CR] = ~ 200 mM; [nanocrystal] = ~ 2 mM). These stock solutions were diluted 10-fold prior to NMR and 1000-fold prior to UV−vis absorption spectroscopy and PLQY measurements. The concentrations of nanocrystals and ligands in benzene-d_6 stock solutions were determined using a combination of NMR and UV−vis absorption spectroscopies according to a previous report.[21] A stock solution of ferrocene (10−25 μL, 0.05 M) was added to a known volume of nanocrystal stock solution and the ferrocene signal used as an internal concentration standard.

Reaction of CdSe−Cd(O$_2$CR)$_2$/HO$_2$CR with CdMe$_2$ or ZnEt$_2$. CdMe$_2$ or ZnEt$_2$ was added (1.7 mg CdMe$_2$, or 1.9 mg ZnEt$_2$) using a microliter syringe to a CdSe stock solution (5 mL) and the solution protected from light. The solution was stirred for 12 h and distilled to dryness under vacuum to remove unreacted CdMe$_2$ or ZnEt$_2$. The residue was dissolved in toluene (5 mL), and methyl acetate (40 mL) was added to precipitate the nanocrystals, which were isolated by centrifugation and decanting the supernatant. The precipitation and centrifugation process was repeated twice and the final nanocrystal powder dried under vacuum before being dissolved in benzene-d_6 for ^{1}H NMR and UV−visible absorption analysis.

Synthesis of CdSe−NH$_2$R′ (R′ = C$_{12}$H$_{25}$, C$_8$H$_{17}$, C$_4$H$_9$). A solution of *n*-octylamine in toluene (5 mL, 4.5 M) was added to a stock solution of CdSe nanocrystals (2 mL, [Cd(O$_2$CR)$_2$] = 0.1 M) and the red solution stirred for 10 min. Methyl acetate (25 mL) was added and the precipitate isolated by centrifugation. This process was repeated 10-fold or until no alkenyl resonance was visible in the ^{1}H NMR spectrum. After the final centrifugation, the nanocrystals were dissolved in toluene, dried under vacuum, and characterized by NMR and UV−visible absorption spectroscopies (see above). If partial precipitation of nanocrystals occurs, 20 μL of primary amine was added to the nanocrystals to aid in redissolution. The photoluminescence quantum yield of isolated CdSe−NH$_2$R′ is 1−2%. *n*-Octylamine ligands were exchanged for *n*-butyl- or *n*-dodecylamine by three rounds of dissolution/precipitation/centrifugation procedure from a 1 M solution of the desired alkylamine in toluene.

Digestion of CdSe−NH$_2$C$_8$H$_{17}$. The volatiles were removed from a stock solution of CdSe−NH$_2$C$_8$H$_{17}$ (500 μL, [nanocrystal] = 0.5−2.3 mM, [NH$_2$C$_8$H$_{17}$] = 0.2−0.3 M) under vacuum over 48 h (this ensures removal of the majority of the octylamine species). Under an argon atmosphere, a 1 mL solution of DCl (2.8 mmol) in D$_2$O and methanol-d_4 (1:1 by volume) was added to this residue. The sample was shaken to mix its components and the mixture gradually dissolved to a clear solution and allowed to stand overnight. The next day, a colorless solution was obtained to which pyridine (10 μL) was added as an internal concentration standard for ^{1}H NMR analysis. The number of aliphatic chains from species other than *n*-octylammonium was estimated from the difference between the integral of the methyl resonance, which measures all aliphatic chains groups, and the integral of the α-CH$_2$ from *n*-octylammonium. Due to the trace amount of organic impurities in these samples, a high concentration of the nanocrystal stock solution is required. Under our conditions, signal-to-noise ratios of the methyl resonance ranged from 100:1 to 1000:1.

Replacement of n-Octylamine Ligands with Cadmium Oleate. A solution of CdSe−NH$_2$C$_8$H$_{17}$ ([nanocrystals] = 2.26 mM) was dried under vacuum for 3 h to remove the volatiles. To this residue was added cadmium oleate dissolved in toluene (2 mL, 0.165 M). The resulting solution was allowed to stir overnight at room temperature and then was purified by precipitation with 10 mL of methyl acetate and centrifugation, affording a red powder that was redissolved in toluene prior to analysis with TEM.

Reaction of Oleic Acid and CdSe−NH$_2$C$_8$H$_{17}$. A stock solution of CdSe−NH$_2$C$_8$H$_{17}$ was diluted with a solution of oleic acid in benzene-d_6 ([nanocrystal] = 0.135 mM, [NH$_2$C$_8$H$_{17}$] = 24 mM, [RCO$_2$H] = 240 mM), and the sample was allowed to sit overnight. The nanocrystals were then purified by three cycles of precipitation with methyl acetate (5 mL), centrifugation, and redissolution. The nanocrystal pellet then dissolved in pentane (5 mL) transferred to a 20 mL vial fitted with a stir bar and placed under vacuum to remove the volatiles. The final nanocrystal powder was dissolved in 1 mL of benzene-d_6 or ^{1}H NMR and UV−vis absorption analysis. Attempts to displace surface bound *n*-octylammonium oleate using *n*-octylamine followed three cycles of precipitation from 4.5 M amine solution according to the procedure described in Synthesis of CdSe−NH$_2$R′.

Reaction of n-Octadecylphosphonic Acid and CdSe−NH$_2$C$_8$H$_{17}$. To a solution of CdSe-NH$_2$C$_8$H$_{17}$ (600 μL, [nanocrystals] = 0.12 mM, [amine] = 21 mM) in a J-Young tube was added 4.28 mg (12.3 μmoles) of *n*-octadecylphosphonic acid. The mixture was sonicated to aid the dissolution of the phosphonic acid and then allowed to react overnight prior to analysis with ^{31}P NMR spectroscopy.

Reaction of Carbon Dioxide and CdSe−NH$_2$C$_8$H$_{17}$. A solution of CdSe-NH$_2$C$_8$H$_{17}$ in toluene-d_8 (600 μL, [nanocrystals] = 0.24 mM, [amine] = 42.7 mM) was placed in a J-Young tube and degassed. Meanwhile, the gas manifold of a Schlenk line was filled with carbon dioxide obtained from the sublimation of dry ice. Carbon dioxide was then admitted to a volumetric gas addition bulb (209 mL) until the internal pressure was 10 Torr as measured with a mercury monometer. This volume of gas was then condensed into the J-Young tube at liquid nitrogen temperature for 5 min. The J-Young tube was then sealed and allowed to warm to room temperature. Addition of isotopically enriched $^{13}CO_2$ (10 μmol) to CdSe-NH$_2$C$_8$H$_{17}$ was performed identically to the procedure described above using a lecture bottle of ^{13}C-labeled carbon dioxide. After the bottle was allowed to stand for 4 h at room temperature, methyl acetate (10 mL) was added and the nanocrystal precipitate isolated by centrifugation. The isolated nanocrystals were further purified by three cycles of dissolution in toluene, precipitation with methyl acetate, and centrifugation.

Reduction of Cadmium Carboxylate Coverage with TMEDA. Reduction of the cadmium carboxylate coverage in CdSe−Cd(O$_2$CR)$_2$ nanocrystal samples was performed following a previously reported method.[21,87] In a typical reaction, CdSe−Cd(O$_2$CR)$_2$ that was previously reacted with ZnEt$_2$ according to Reaction of CdSe−Cd(O$_2$CR)$_2$ with CdMe$_2$ or ZnEt$_2$ was dissolved in 5 mL of neat TMEDA and allowed to stir for 10 min. The solution was then precipitated with 25 mL of methyl acetate, and the nanocrystals were isolated by centrifugation. The clear supernatant was discarded and the pellet subjected to two additional cycles of TMEDA/methyl acetate/centrifugation. The nanocrystals were then separated from adventitious TMEDA by two cycles of dissolution in toluene (5 mL), precipitation with methyl acetate (25 mL), and centrifugation. The resulting nanocrystals were insoluble in pentane but could be redispersed in toluene or benzene.

Binding of Oleic Acid to CdSe−Cd(O$_2$CR)$_2$ with Reduced Oleate Coverage. In a typical reaction, to a stock solution of CdSe−Cd(O$_2$CR)$_2$ (500 μL, [nanocrystals] = 0.48 mM, [Cd(O$_2$CR)$_2$] = 0.013 M, 0.53 carboxylates nm^{-2}) that had previously been treated with TMEDA according to Reduction of Cadmium Carboxylate Coverage with TMEDA in either benzene-d_6 or tetrachloroethylene was added oleic acid (12 μL, 394 equiv per nanocrystal), and the solution was allowed to stir for 3 h. The nanocrystals were then precipitated by addition of methyl acetate (10 mL) and isolated by centrifugation. The red pellet was then purified by five cycles of dissolution in pentane (1 mL), precipitation with methyl acetate (10 mL), and centrifugation. The nanocrystals were then dispersed in benzene-d_6 for NMR spectroscopy.

■ ASSOCIATED CONTENT

Supporting Information

The Supporting Information is available free of charge on the ACS Publications website at DOI: 10.1021/jacs.6b13234.

Additional reaction schemes, FTIR, NMR, and UV−vis absorption spectra of selected nanocrystal samples and control experiments; ^{1}H NMR spectra of digested nanocrystal samples; DOSY; comparisons of different cleaning methods; TEM images; and DLS measurements (PDF)

DOI: 10.1021/jacs.6b13234
J. Am. Chem. Soc. 2017, 139, 3227−3236

AUTHOR INFORMATION

Corresponding Author

*jso2115@columbia.edu

ORCID

Peter E. Chen: 0000-0001-6933-367X

Jonathan S. Owen: 0000-0001-5502-3267

Notes

The authors declare no competing financial interest.

ACKNOWLEDGMENTS

This work was funded by the Department of Energy under Grant No. DE-SC0006410. P.E.C. and N.C.A. acknowledge support from the National Science Foundation under Grant Nos. DGE11-44155 and DGE07-07425, respectively. Jonathan De Roo is acknowledged for his assistance in DOSY analysis. Ilan Jen-La Plante is acknowledged for providing the TEM, which was conducted at the New York Structural Biology Center constructed with support from Research Facilities Improvement Program Grant No. C06 RR017528-01-CEM from the National Center for Research Resources, National Institutes of Health.

REFERENCES

(1) Owen, J. *Science* **2015**, *347* (6222), 615−6.

(2) De Roo, J.; Justo, Y.; De Keukeleere, K.; Van den Broeck, F.; Martins, J. C.; Van Driessche, I.; Hens, Z. *Angew. Chem., Int. Ed.* **2015**, *54* (22), 6488−91.

(3) Doris, S. E.; Lynch, J. J.; Li, C.; Wills, A. W.; Urban, J. J.; Helms, B. A. *J. Am. Chem. Soc.* **2014**, *136* (44), 15702−10.

(4) Rosen, E. L.; Buonsanti, R.; Llordes, A.; Sawvel, A. M.; Milliron, D. J.; Helms, B. A. *Angew. Chem., Int. Ed.* **2012**, *51* (3), 684−9.

(5) Caldwell, M. A.; Albers, A. E.; Levy, S. C.; Pick, T. E.; Cohen, B. E.; Helms, B. A.; Milliron, D. J. *Chem. Commun.* **2011**, *47* (1), 556−8.

(6) Dong, A.; Ye, X.; Chen, J.; Kang, Y.; Gordon, T.; Kikkawa, J. M.; Murray, C. B. *J. Am. Chem. Soc.* **2011**, *133* (4), 998−1006.

(7) Hughes, B. K.; Ruddy, D. A.; Blackburn, J. L.; Smith, D. K.; Bergren, M. R.; Nozik, A. J.; Johnson, J. C.; Beard, M. C. *ACS Nano* **2012**, *6* (6), 5498−506.

(8) Kim, D. K.; Fafarman, A. T.; Diroll, B. T.; Chan, S. H.; Gordon, T. R.; Murray, C. B.; Kagan, C. R. *ACS Nano* **2013**, *7* (10), 8760−70.

(9) Turo, M. J.; Macdonald, J. E. *ACS Nano* **2014**, *8* (10), 10205−13.

(10) Anderson, N. C.; Owen, J. S. *Chem. Mater.* **2013**, *25*, 69−76.

(11) Zhang, H.; Jang, J.; Liu, W.; Talapin, D. V. *ACS Nano* **2014**, *8* (7), 7359−69.

(12) Tang, J.; Kemp, K. W.; Hoogland, S.; Jeong, K. S.; Liu, H.; Levina, L.; Furukawa, M.; Wang, X.; Debnath, R.; Cha, D.; Chou, K. W.; Fischer, A.; Amassian, A.; Asbury, J. B.; Sargent, E. H. *Nat. Mater.* **2011**, *10* (10), 765−71.

(13) Nag, A.; Kovalenko, M. V.; Lee, J. S.; Liu, W.; Spokoyny, B.; Talapin, D. V. *J. Am. Chem. Soc.* **2011**, *133* (27), 10612−20.

(14) Oh, S. J.; Berry, N. E.; Choi, J. H.; Gaulding, E. A.; Paik, T.; Hong, S. H.; Murray, C. B.; Kagan, C. R. *ACS Nano* **2013**, *7* (3), 2413−21.

(15) Liu, Y.; Tolentino, J.; Gibbs, M.; Ihly, R.; Perkins, C. L.; Liu, Y.; Crawford, N.; Hemminger, J. C.; Law, M. *Nano Lett.* **2013**, *13* (4), 1578−87.

(16) Kovalenko, M. V.; Manna, L.; Cabot, A.; Hens, Z.; Talapin, D. V.; Kagan, C. R.; Klimov, V. I.; Rogach, A. L.; Reiss, P.; Milliron, D. J.; Guyot-Sionnnest, P.; Konstantatos, G.; Parak, W. J.; Hyeon, T.; Korgel, B. A.; Murray, C. B.; Heiss, W. *ACS Nano* **2015**, *9* (2), 1012−57.

(17) Talapin, D. V.; Lee, J.-S.; Kovalenko, M. V.; Shevchenko, E. V. *Chem. Rev.* **2010**, *110*, 389−458.

(18) Wang, F.; Tang, R.; Buhro, W. E. *Nano Lett.* **2008**, *8* (10), 3521−4.

(19) Belman, N.; Israelachvili, J. N.; Li, Y.; Safinya, C. R.; Bernstein, J.; Golan, Y. *Nano Lett.* **2009**, *9* (5), 2088−93.

(20) Luo, B.; Rossini, J. E.; Gladfelter, W. L. *Langmuir* **2009**, *25* (22), 13133−41.

(21) Anderson, N. C.; Hendricks, M. P.; Choi, J. J.; Owen, J. S. *J. Am. Chem. Soc.* **2013**, *135* (49), 18536−48.

(22) Kim, W.; Lim, S. J.; Jung, S.; Shin, S. K. *J. Phys. Chem. C* **2010**, *114* (3), 1539−1546.

(23) Lefrançois, A.; Couderc, E.; Faure-Vincent, J.; Sadki, S.; Pron, A.; Reiss, P. *J. Mater. Chem.* **2011**, *21* (31), 11524.

(24) Ji, X.; Copenhaver, D.; Sichmeller, C.; Peng, X. *J. Am. Chem. Soc.* **2008**, *130* (17), 5726−35.

(25) Zillner, E.; Fengler, S.; Niyamakom, P.; Rauscher, F.; Kohler, K.; Dittrich, T. *J. Phys. Chem. C* **2012**, *116* (31), 16747−16754.

(26) Yu, D.; Wang, C.; Guyot-Sionnest, P. *Science* **2003**, *300* (5623), 1277−1280.

(27) Hanrath, T.; Veldman, D.; Choi, J. J.; Christova, C. G.; Wienk, M. M.; Janssen, R. A. *ACS Appl. Mater. Interfaces* **2009**, *1* (2), 244−50.

(28) Kuno, M.; Lee, J. K.; Dabbousi, B. O.; Mikulec, F. V.; Bawendi, M. G. *J. Chem. Phys.* **1997**, *106* (23), 9869−9882.

(29) Lokteva, I.; Radychev, N.; Witt, F.; Borchert, H.; Parisi, J.; Kolny-Olesiak, J. *J. Phys. Chem. C* **2010**, *114* (29), 12784−12791.

(30) Photolysis of CdSe−$Cd(O_2CR)_2$/$CdMe_2$ also induces the precipitation of a gray powder that is assumed to be cadmium metal.

(31) Wehrenberg, B. L.; Guyot-Sionnest, P. *J. Am. Chem. Soc.* **2003**, *125* (26), 7806−7.

(32) Guyot-Sionnest, P.; Wehrenberg, B.; Yu, D. *J. Chem. Phys.* **2005**, *123* (7), 074709.

(33) Rinehart, J. D.; Schimpf, A. M.; Weaver, A. L.; Cohn, A. W.; Gamelin, D. R. *J. Am. Chem. Soc.* **2013**, *135* (50), 18782−5.

(34) Schimpf, A. M.; Knowles, K. E.; Carroll, G. M.; Gamelin, D. R. *Acc. Chem. Res.* **2015**, *48* (7), 1929−37.

(35) Shim, M.; Guyot-Sionnest, P. *Nature* **2000**, *407* (6807), 981−3.

(36) Tsui, E. Y.; Hartstein, K. H.; Gamelin, D. R. *J. Am. Chem. Soc.* **2016**, *138* (35), 11105−8.

(37) Orchard, K. L.; White, A. J. P.; Shaffer, M. S. P.; Williams, C. K. *Organometallics* **2009**, *28* (19), 5828−5832.

(38) Tang, H.; Richey, H. G. *Organometallics* **2001**, *20* (8), 1569−1574.

(39) Turner, C. J.; White, R. F. M. *J. Magn. Reson.* **1977**, *26* (1), 1−5.

(40) Sinclair, R. G.; Mckay, A. F.; Myers, G. S.; Jones, R. N. *J. Am. Chem. Soc.* **1952**, *74* (10), 2578−2585.

(41) Digestion of CdSe−NH_2R' in DCl/CD_3OD verified the absence of carboxylic acid ligands, although other organic fragments derived from C18 chains were isolated and characterized by mass spectrometry. One to three of these impurities per nanocrystal are present in the isolated product (Figure S8) that may result from side reactions between SeO_2 and 1-octadecene during the precursor conversion.

(42) This displacement of only 75% of the cadmium carboxylate is in contrast to our previously reported results where these amine concentrations should displace > 95% of the cadmium carboxylate from the nanocrystal surface. We propose that this discrepancy is due to a higher concentration of nanocrystals and cadmium carboxylate in this report relative to these past results (whereas we previously performed these in situ ^1H NMR studies with a carboxylate concentration of 0.02 M, these samples had a concentration of 0.1 M).

(43) Typical [nanocrystal] used in this study are 2−5 mM, corresponding to 50−125 amines per nanocrystal at [amine] = 0.1 M, or a maximum coverage ~3 amines nm^{-2} assuming all amines present are bound to the nanocrystal.

(44) De Roo, J.; Van den Broeck, F.; De Keukeleere, K.; Martins, J. C.; Van Driessche, I.; Hens, Z. *J. Am. Chem. Soc.* **2014**, *136* (27), 9650−7.

(45) Chalmers, J. M.; Griffiths, P. R. *Handbook of Vibrational Spectroscopy*; John Wiley & Sons: Chichester, U, 2001.

(46) Cox, B. G. *Acids and Bases: Solvent Effects on Acid−Base Strength*; Oxford University Press, 2013.

DOI: 10.1021/jacs.6b13234
J. Am. Chem. Soc. 2017, 139, 3227−3236

(47) Izutsu, K. *Acid−base Dissociation Constants in Dipolar Aprotic Solvents*; Blackwell Scientific Publications, 1990.
(48) Barrow, G. M.; Yerger, E. A. *J. Am. Chem. Soc.* **1954**, *76* (20), 5211−5216.
(49) De Roo, J.; Ibanez, M.; Geiregat, P.; Nedelcu, G.; Walravens, W.; Maes, J.; Martins, J. C.; Van Driessche, I.; Kovalenko, M. V.; Hens, Z. *ACS Nano* **2016**, *10* (2), 2071−81.
(50) Dierick, R.; Van den Broeck, F.; De Nolf, K.; Zhao, Q.; Vantomme, A.; Martins, J. C.; Hens, Z. *Chem. Mater.* **2014**, *26* (20), 5950−5957.
(51) Campos, M. P.; Owen, J. S. *Chem. Mater.* **2016**, *28* (1), 227−233.
(52) Heath, J. R. *Chem. Soc. Rev.* **1998**, *27* (1), 65−71.
(53) Demmer, C. S.; Krogsgaard-Larsen, N.; Bunch, L. *Chem. Rev.* **2011**, *111* (12), 7981−8006.
(54) Wang, F.; Tang, R.; Kao, J. L.; Dingman, S. D.; Buhro, W. E. *J. Am. Chem. Soc.* **2009**, *131* (13), 4983−94.
(55) Owen, J. S.; Park, J.; Trudeau, P. E.; Alivisatos, A. P. *J. Am. Chem. Soc.* **2008**, *130* (37), 12279−81.
(56) Gomes, R.; Hassinen, A.; Szczygiel, A.; Zhao, Q. A.; Vantomme, A.; Martins, J. C.; Hens, Z. *J. Phys. Chem. Lett.* **2011**, *2* (3), 145−152.
(57) Frasco, D. L. *J. Chem. Phys.* **1964**, *41* (7), 2134−2140.
(58) The $\nu(NCO_2)$ of the carbamate anion cannot be seen due to N−H and C−H bending modes of the amine ligands.
(59) A vibrational band from water is also observed unless the added oleic acid or carbon dioxide are anhydrous.
(60) The remaining *n*-octylammonium oleate ligands could be removed by adding excess $ZnEt_2$ (Figure S18). In this case, a slight blue shift in the UV−vis absorption and the formation of $CdEt_2$ (Figure S19 and S20) were observed, indicating cation exchange between Cd^{2+} and Zn^{2+} in the nanocrystal. The different reactivity, compared to what is observed with CdSe−$Cd(O_2CR)_2$/HO_2CR, may result from polymeric zinc amides that form in a side reaction between *n*-octylamine and $ZnEt_2$.
(61) Voznyy, O. *J. Phys. Chem. C* **2011**, *115* (32), 15927−15932.
(62) Margraf, J. T.; Ruland, A.; Sgobba, V.; Guldi, D. M.; Clark, T. *Langmuir* **2013**, *29* (49), 15450−6.
(63) Sharghi, N.; Lalezari, I. *Spectrochim. Acta* **1964**, *20* (2), 237−238.
(64) Brown, G. E.; Henrich, V. E.; Casey, W. H.; Clark, D. L.; Eggleston, C.; Felmy, A.; Goodman, D. W.; Gratzel, M.; Maciel, G.; McCarthy, M. I.; Nealson, K. H.; Sverjensky, D. A.; Toney, M. F.; Zachara, J. M. *Chem. Rev.* **1999**, *99* (1), 77−174.
(65) Westall, J.; Hohl, H. *Adv. Colloid Interface Sci.* **1980**, *12* (4), 265−294.
(66) Haworth, A. *Adv. Colloid Interface Sci.* **1990**, *32* (1), 43−78.
(67) Hansen, J. P.; Lowen, H. *Annu. Rev. Phys. Chem.* **2000**, *51*, 209−42.
(68) Dirin, D. N.; Dreyfuss, S.; Bodnarchuk, M. I.; Nedelcu, G.; Papagiorgis, P.; Itskos, G.; Kovalenko, M. V. *J. Am. Chem. Soc.* **2014**, *136* (18), 6550−3.
(69) Fafarman, A. T.; Koh, W. K.; Diroll, B. T.; Kim, D. K.; Ko, D. K.; Oh, S. J.; Ye, X.; Doan-Nguyen, V.; Crump, M. R.; Reifsnyder, D. C.; Murray, C. B.; Kagan, C. R. *J. Am. Chem. Soc.* **2011**, *133* (39), 15753−61.
(70) Dolzhnikov, D. S.; Zhang, H.; Jang, J.; Son, J. S.; Panthani, M. G.; Shibata, T.; Chattopadhyay, S.; Talapin, D. V. *Science* **2015**, *347* (6220), 425−8.
(71) Kovalenko, M. V.; Scheele, M.; Talapin, D. V. *Science* **2009**, *324*, 1417−1420.
(72) Cheng, W. L.; Dong, S. J.; Wang, E. K. *Langmuir* **2003**, *19* (22), 9434−9439.
(73) Mattoussi, H.; Cumming, A. W.; Murray, C. B.; Bawendi, M. G.; Ober, R. *J. Chem. Phys.* **1996**, *105* (22), 9890−9896.
(74) Murray, C. B.; Norris, D. J.; Bawendi, M. G. *J. Am. Chem. Soc.* **1993**, *115*, 8706−8715.
(75) Valdez, C. N.; Schimpf, A. M.; Gamelin, D. R.; Mayer, J. M. *ACS Nano* **2014**, *8* (9), 9463−70.
(76) Norman, Z. M.; Anderson, N. C.; Owen, J. S. *ACS Nano* **2014**, *8* (7), 7513−21.
(77) Asensio, J. M.; Tricard, S.; Coppel, Y.; Andres, R.; Chaudret, B.; de Jesus, E. *Angew. Chem., Int. Ed.* **2016**, DOI: 10.1002/anie.201610251.
(78) Ernst, J. B.; Muratsugu, S.; Wang, F.; Tada, M.; Glorius, F. *J. Am. Chem. Soc.* **2016**, *138* (34), 10718−21.
(79) Lu, H.; Zhou, Z.; Prezhdo, O. V.; Brutchey, R. L. *J. Am. Chem. Soc.* **2016**, *138* (45), 14844−14847.
(80) Liu, W.; Greytak, A. B.; Lee, J.; Wong, C. R.; Park, J.; Marshall, L. F.; Jiang, W.; Curtin, P. N.; Ting, A. Y.; Nocera, D. G.; Fukumura, D.; Jain, R. K.; Bawendi, M. G. *J. Am. Chem. Soc.* **2010**, *132* (2), 472−83.
(81) Koczkur, K. M.; Mourdikoudis, S.; Polavarapu, L.; Skrabalak, S. E. *Dalton Trans.* **2015**, *44* (41), 17883−905.
(82) Sun, Y. G.; Mayers, B.; Herricks, T.; Xia, Y. N. *Nano Lett.* **2003**, *3* (7), 955−960.
(83) Xia, X.; Zeng, J.; Oetjen, L. K.; Li, Q.; Xia, Y. *J. Am. Chem. Soc.* **2012**, *134* (3), 1793−801.
(84) Anderson, N. C. *The Surface Chemistry of Metal Chalcogenide Nanocrystals*; Columbia University, 2014.
(85) Kosolapoff, G. M. *J. Am. Chem. Soc.* **1945**, *67* (7), 1180−1182.
(86) Chen, O.; Chen, X.; Yang, Y.; Lynch, J.; Wu, H.; Zhuang, J.; Cao, Y. C. *Angew. Chem., Int. Ed.* **2008**, *47* (45), 8638−41.
(87) Busby, E.; Anderson, N. C.; Owen, J. S.; Sfeir, M. Y. *J. Phys. Chem. C* **2015**, *119* (49), 27797−27803.

DOI: 10.1021/jacs.6b13234
J. Am. Chem. Soc. 2017, 139, 3227−3236